



**HAL**  
open science

**Class-A operation of an optically-pumped 1.6  
 $\mu\text{m}$ -emitting quantum dash-based  
vertical-external-cavity surface-emitting laser on InP**

Salvatore Pes, Cyril Paranthoen, Christophe Levallois, Nicolas Chevalier,  
Cyril Hamel, Kevin Audo, Goulc'Hen Loas, Steve Bouhier, Carmen Gomez,  
Jean-Christophe Harmand, et al.

► **To cite this version:**

Salvatore Pes, Cyril Paranthoen, Christophe Levallois, Nicolas Chevalier, Cyril Hamel, et al.. Class-A operation of an optically-pumped 1.6  $\mu\text{m}$ -emitting quantum dash-based vertical-external-cavity surface-emitting laser on InP. Optics Express, 2017, OSA Optics Express, 25 (10), pp.11760-11766. 10.1364/OE.25.011760 . hal-01533213

**HAL Id: hal-01533213**

**<https://hal.science/hal-01533213>**

Submitted on 6 Jun 2017

**HAL** is a multi-disciplinary open access archive for the deposit and dissemination of scientific research documents, whether they are published or not. The documents may come from teaching and research institutions in France or abroad, or from public or private research centers.

L'archive ouverte pluridisciplinaire **HAL**, est destinée au dépôt et à la diffusion de documents scientifiques de niveau recherche, publiés ou non, émanant des établissements d'enseignement et de recherche français ou étrangers, des laboratoires publics ou privés.

# Class-A Operation of an Optically-Pumped 1.6 $\mu\text{m}$ -emitting Quantum Dash-based Vertical-External-Cavity Surface-Emitting Laser on InP

SALVATORE PES,<sup>1\*</sup> CYRIL PARANTHOËN,<sup>1</sup> CHRISTOPHE LEVALLOIS,<sup>1</sup>  
NICOLAS CHEVALIER,<sup>1</sup> CYRIL HAMEL,<sup>1</sup> KEVIN AUDDO,<sup>1</sup> GOULC'HEN LOAS,<sup>1</sup>  
STEVE BOUHIER,<sup>1</sup> CARMEN GOMEZ,<sup>2</sup> JEAN-CHRISTOPHE HARMAND,<sup>2</sup>  
SOPHIE BOUCHOULE,<sup>2</sup> HERVÉ FOLLIOT,<sup>1</sup> AND MEHDI ALOUINI<sup>1</sup>

<sup>1</sup>UMR FOTON, CNRS, INSA de Rennes, Université de Rennes 1, F-35708 Rennes, France

<sup>2</sup>Centre de Nanosciences et de Nanotechnologies, CNRS, Université Paris-Sud, 91360 Marcoussis, France

\*salvatore.pes@insa-rennes.fr

**Abstract:** A continuous-wave 1.6  $\mu\text{m}$ -emitting InAs Quantum Dash-based Optically-Pumped Vertical-External-Cavity Surface-Emitting Laser on InP is demonstrated. The laser emits in the L-band with a stable linear polarization. Up to 163 mW output power has been obtained in multi-transverse mode regime. Single-frequency regime is achieved in the 1609-1622 nm range, with an estimated linewidth of 22 kHz in a 49 mm cavity, and a maximum emitted power of 7.9 mW at 1611 nm. In such conditions, the laser exhibits a Class-A behavior, with a cut-off frequency of 800 kHz and a shot-noise floor of -158 dB/Hz for 2 mA of detected photocurrent.

© 2017 Optical Society of America

**OCIS codes:** (140.5960) Semiconductor lasers; (140.7260) Vertical cavity surface emitting lasers; (230.5590) Quantum-well, -wire and -dot devices; (270.2500) Fluctuations, relaxations, and noise; (350.4010) Microwaves.

## References and links

1. M. Kuznetsov, F. Hakimi, R. Sprague, and A. Mooradian, "High-power (>0.5-W CW) diode-pumped vertical-external-cavity surface-emitting semiconductor lasers with circular TEM<sub>00</sub> beams," *IEEE Photon. Technol. Lett.* **9**(8), 1063-1065 (1997).
2. O. G. Okhotnikov, *Semiconductor Disk Lasers* (Wiley-VCH, 2010).
3. A. Rahimi-Iman, "Recent advances in VECSELS," *J. Opt.* **18**(9), 093003 (2016).
4. F. Zhang, B. Heinen, M. Wichmann, C. Möller, B. Kunert, A. Rahimi-Iman, W. Stolz, and M. Koch, "A 23-watt single-frequency vertical-external-cavity surface-emitting laser," *Opt. Express* **22**(11), 12817-12822 (2014).
5. L. Chaccour, G. Aubin, K. Merghem, J.-L. Oudar, A. Khadour, P. Chatellier, and S. Bouchoule, "Cross-Polarized Dual-Frequency VECSEL at 1.5  $\mu\text{m}$  for Fiber-Based Sensing Applications," *IEEE Photon. J.* **8**(6), 1-10 (2016).
6. D. Waldburger, S. M. Link, M. Mangold, C. G. E. Alfieri, E. Gini, M. Golling, B. W. Tilma, and U. Keller, "High-power 100 fs semiconductor disk lasers," *Optica* **3**(8), 844-852 (2016).
7. P. Cermak, M. Triki, A. Garnache, L. Cerutti and D. Romanini, "Optical-Feedback Cavity-Enhanced Absorption Spectroscopy Using a Short-Cavity Vertical-External-Cavity Surface-Emitting Laser," *IEEE Photon. Technol. Lett.* **22**(21), 1607-1609 (2010).
8. E. J. Saarinen, J. Lyytikäinen, S. Ranta, A. Rantamäki, A. Sirbu, V. Iakovlev, E. Kapon, and O. G. Okhotnikov, "750 nm 1.5 W frequency-doubled semiconductor disk laser with a 44 nm tuning range," *Opt. Lett.* **40**(19), 4380-4383 (2015).
9. P. Dumont, F. Camargo, J.-M. Danet, D. Holleville, S. Guerandel, G. Pillet, G. Baili, L. Morvan, D. Dolfi, I. Gozhyk, G. Beaudoin, I. Sagnes, P. Georges, and G. Lucas-Leclin, "Low-Noise Dual-Frequency Laser for Compact Cs Atomic Clocks," *J. Lightwave Technol.* **32**(20), 3817-3823 (2014).
10. S. De, G. Baili, M. Alouini, J. Harmand, S. Bouchoule, and F. Bretenaker, "Class-A dual-frequency VECSEL at telecom wavelength," *Opt. Lett.* **39**(19), 5586-5589 (2014).
11. G. Baili, L. Morvan, G. Pillet, S. Bouchoule, Z. Zhao, J. Oudar, L. Ménager, S. Formont, F. Van Dijk, M. Faugeron, M. Alouini, F. Bretenaker, and D. Dolfi, "Ultralow Noise and High-Power VECSEL for High Dynamic Range and Broadband RF/Optical Links," *J. Lightwave Technol.* **32**(20), 3489-3494 (2014).
12. G. Baili, M. Alouini, D. Dolfi, F. Bretenaker, I. Sagnes, and A. Garnache, "Shot-noise-limited operation of a monomode high-cavity-finesse semiconductor laser for microwave photonics applications," *Opt. Lett.* **32**(6), 650-652 (2007).

13. M. Z. M. Khan, T. K. Ng, B. S. Ooi, "Self-assembled InAs/InP quantum dots and quantum dashes: Material structures and devices", *Progress in Quantum Electronics* **38**(6), 237-313 (2014).
14. F. Lelarge, B. Dagens, J. Renaudier, R. Brenot, A. Accard, F. v. Dijk, D. Make, O. L. Gouezigou, J. G. Provost, F. Poingt, J. Landreau, O. Drisse, E. Derouin, B. Rousseau, F. Pommereau, G. H. Duan, "Recent Advances on InAs/InP Quantum Dash Based Semiconductor Lasers and Optical Amplifiers Operating at 1.55  $\mu\text{m}$ ," *IEEE J. Sel. Topics Quantum Electron.* **13**(1), 111-124 (2007).
15. J. M. Lamy, C. Paranthoën, C. Levallois, A. Nakkar, H. Folliot, J. P. Gauthier, O. Dehaese, A. Le Corre, and S. Loualiche, "Polarization control of 1.6 $\mu\text{m}$  vertical-cavity surface-emitting lasers using InAs quantum dashes on InP(001)," *Appl. Phys. Lett.* **95**(1), 011117 (2009).
16. J.-P. Gauthier, C. Paranthoën, C. Levallois, A. Shuaib, J.-M. Lamy, H. Folliot, M. Perrin, O. Dehaese, N. Chevalier, O. Durand, and A. Le Corre, "Enhancement of the polarization stability of a 1.55  $\mu\text{m}$  emitting vertical-cavity surface-emitting laser under modulation using quantum dashes," *Opt. Express* **20**(15), 16832-16837 (2012).
17. F. Taleb, C. Levallois, C. Paranthoën, J.-P. Gauthier, N. Chevalier, M. Perrin, Y. Léger, O. De Sagazan, A. Le Corre, "VCSEL Based on InAs Quantum-Dashes With a Lasing Operation Over a 117-nm Wavelength Span," *IEEE Photon. Technol. Lett.* **25**(21), 2126-2128 (2013).
18. J. Boucart, F. Gaborit, C. Fortin, L. Goldstein, J. Jacquet, K. Leifer, "Optimization of the metamorphic growth of GaAs for long wavelength VCSELs," *J. Cryst. Growth* **201-202**, 1015-1019 (1999).
19. Z. Zhao, S. Bouchoule, J. Song, E. Galopin, J.-C. Harmand, J. Decobert, G. Aubin, and J.-L. Oudar, "Subpicosecond pulse generation from a 1.56  $\mu\text{m}$  mode-locked VECSEL," *Opt. Lett.* **36**(22), 4377-4379 (2011).
20. L. Richter, H. Mandelberg, M. Kruger and P. McGrath, "Linewidth determination from self-heterodyne measurements with subcoherence delay times," *IEEE J. Quantum Electron.* **22**(11), 2070-2074 (1986).
21. B. Jacobsson, V. Pasiskevicius, and F. Laurell, "Tunable single-longitudinal-mode ErYb:glass laser locked by a bulk glass Bragg grating," *Opt. Lett.* **31**(11), 1663-1665 (2006).
22. A. Rantamäki, J. Rautiainen, A. Sirbu, A. Mereuta, E. Kapon, and O. G. Okhotnikov, "1.56  $\mu\text{m}$  1 watt single frequency semiconductor disk laser," *Opt. Express* **21**(2), 2355-2360 (2013).
23. R. Nagarajan, S. Levy, A. Mar and J. E. Bowers, "Resonantly enhanced semiconductor lasers for efficient transmission of millimeter wave modulated light," *IEEE Photon. Technol. Lett.* **5**(1), 4-6 (1993).
24. G. Baili, M. Alouini, T. Malherbe, D. Dolfi, I. Sagnes and F. Bretenaker, "Direct observation of the class-B to class-A transition in the dynamical behavior of a semiconductor laser," *Europhys. Lett.* **87**(4), 44005 (2009).

## 1. Introduction

Since the first demonstration of room-temperature continuous-wave high-power emission in 1997 [1], Vertical-External-Cavity Surface-Emitting Lasers (VECSELs, also known as Semiconductor Disk Lasers, SDLs) have emerged as original devices, capable to ensure high quality circular beams and narrow linewidth, with relatively high power levels, which are typical of solid-state lasers, together with the advantages of semiconductor lasers, such as wide spectral coverage through bandgap engineering and the possibility of electrical injection [2,3].

Thanks to their optical properties and versatility, VECSELs are currently used in a wide range of applications, such as high-power high-quality laser sources [4], fiber sensors [5], ultrafast photonics [6], gas sensing and molecular spectroscopy [7], biomedicine [8], metrology [9] and microwave photonics [10,11]. In the case of microwave or millimeter-wave signal generation, strict constraints are set on the spectral purity of the optical sources, requiring low-intensity noise levels over a wide frequency range. Moreover, tunability is highly desired in such systems. In the past, VECSELs have already been demonstrated to show interesting features as low-noise optical sources, provided that they are operated in the so-called Class-A regime, i.e. without the appearance of relaxation oscillations [12]. This can be achieved with high-finesse and sufficiently long laser cavities that ensure a photon lifetime much longer than the active medium carrier lifetime, leading to an overdamped laser dynamic operation typical of first-order systems, which is free of resonant phenomena.

On the other hand, as a result of the advantages offered by the quantification of low-dimensional quantum systems in terms of lower threshold current, broader gain response or improved thermal stability with respect to quantum wells, quantum dash-based active media have been extensively studied in the past [13]. Most of the contributions presented in the literature are related to edge-emitting and mode-locked lasers or semiconductor optical amplifiers [13,14], with some works on micrometer-long-cavity VCSELs, for which a well-

defined and stable linear state-of-polarization [15,16], and a very wide gain bandwidth [17] were reported. It is thus interesting to investigate the behavior of such nanostructured semiconductor active medium in an external-cavity configuration, in order to benefit from the long-cavity setup in terms of laser linewidth and intensity noise performances. In this paper, the design and the characterization of a continuous-wave 1.6  $\mu\text{m}$ -emitting Optically-Pumped InAs Quantum-Dash-based Vertical-External-Cavity Surface-Emitting Laser (OP-QDH-VECSEL) on InP substrate is discussed. Room-temperature output power characteristics and emission spectra are presented, together with laser linewidth estimation and phase noise measurements in free-running operation. Finally, Class-A operation is demonstrated on such a laser.

## 2. Laser design and characterization

The detailed structure of the OP-QDH-VECSEL chip is illustrated in Fig. 1(a). The active medium has been grown by Gas-Source Molecular Beam Epitaxy (RIBER 32 system) on a (001)-oriented InP substrate and consists of three sets of six planes of self-assembled InAs quantum dashes (QDH). Each QDH layer is separated by 15-nm-thick  $\text{In}_{0.8}\text{Ga}_{0.2}\text{As}_{0.435}\text{P}_{0.565}$  quaternary alloy barriers and surrounded by thicker quaternary alloy layers, which ensure the photo-generated carriers confinement and enhance the pump absorption. The thickness of such layers has been chosen to provide a homogenous excitation of the active region. The structure has been designed in order to accommodate the three sets at the antinodes of the stationary electric field thanks to InP spacers, in the so-called Resonant Periodic Gain configuration. Figure 1(b) shows a  $2 \times 2 \mu\text{m}^2$  atomic force microscope (AFM) image of the last uncapped plane from a set of six QDH layers. It shows uniformly aligned QDH nanostructures along the [1-10] crystallographic axis, which provide a stable linearly-polarized emitted light along the QDH growth direction [15]. Figure 1(c) shows the room-temperature polarization-resolved photoluminescence (PL) spectra of a typical QDH active region along the [1-10] (red dashed curve) and [110] (blue dotted curve) directions, confirming the polarization properties of QDH-based active regions. If compared to strained quantum wells (SQWs) active media (solid black curve), the size dispersion of such elongated nanostructures gives rise to a broader emission, with comparable integrated PL values. Further information about InAs quantum dash growth and morphology can be found in [15]. The OP-QDH-VECSEL has been completed by a bottom hybrid Distributed Bragg Reflector, consisting of 17 pairs of GaAs/ $\text{Al}_{0.97}\text{Ga}_{0.03}\text{As}$  layers, which have been metamorphically grown by MBE on the active region [18], and a gold metallic layer. After a metallic bonding onto a CVD-grade diamond host substrate in a flip-chip configuration [19], the InP substrate has been chemically removed and the whole device has been fixed on a thermally-controlled copper heat-sink. A  $\text{SiN}_x$  anti-reflection (AR) coating at the emission wavelength ( $\sim 1600 \text{ nm}$ ) has been finally deposited on the top surface. On one hand the AR coating leads to a lower value of the maximum modal gain, due to a reduction of the micro-cavity resonance, on the other hand it allows to get a nearly constant modal gain on a broader wavelength range. The laser performances are therefore less sensitive to wavelength variations due to micro-cavity tuning, thermal shift or filtering effects introduced by the extended cavity configuration.

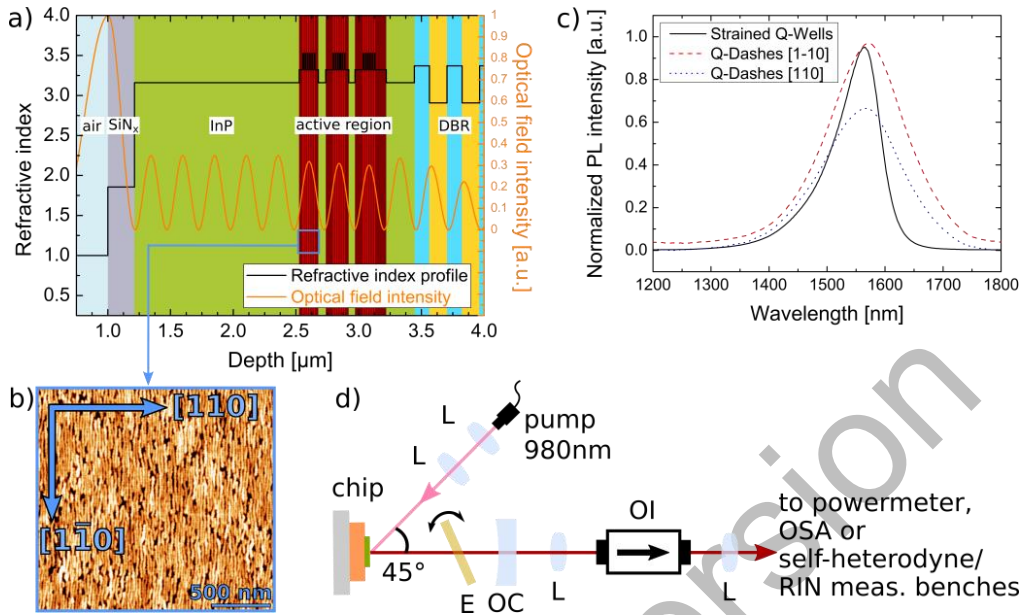


Fig. 1. (a) OP-QDH-VECSEL structure and internal optical field intensity. (b)  $2 \times 2 \mu\text{m}^2$  AFM image of the last uncapped plane from a set of six QDH layers. (c) Normalized room-temperature polarization-resolved PL spectra of SQW-based and QDH-based active regions (6 planes each). (d) Cavity setup (L: lens, E: etalon, OC: output coupler, OI: optical isolator).

The device has been characterized using the experimental setup depicted in Fig. 1(d). The QDH-VECSEL chip has been assembled with a concave output mirror to form the laser cavity. Initially, an output coupler with a radius of curvature ( $R_{OC}$ ) of 15 mm and a reflectivity value of  $R = 99.2\%$  at 1600 nm has been used to characterize our device. The cavity length has been set to 12 mm. The active medium has been continuously pumped by a multi-mode 980 nm semiconductor laser diode placed at an incidence angle of  $45^\circ$  with respect to the cavity axis, giving an elliptical pump spot size of about  $145 \mu\text{m} \times 210 \mu\text{m}$  on the chip surface. Under such conditions, the QDH-VECSEL was operating in the multi-longitudinal mode regime (switching from a mono-transverse to a multi-transverse mode emission, at a pump power around 4 W), with a continuous wave (CW) maximum output power of 163 mW at  $T = 20^\circ\text{C}$  (pump limited), as shown in Fig. 2(a). Two multi-mode emission spectra are also presented in Fig. 2(a), for two different incident pump power values (just above and far from the threshold, respectively), showing a typical redshift from 1611 nm to 1619 nm (central wavelength) attributed to thermal effects, and a broadening related to the appearance of higher-transverse and longitudinal modes. This measurement gives an idea of the potential power and spectral width achievable with this QDH-VECSEL. In a second step, the cavity length has been extended to 49 mm (output coupler with  $R_{OC} = 50$  mm and  $R = 99.5\%$  at 1600 nm) and the active medium has been pumped by a 980 nm fiber-Bragg-grating (FBG) stabilized single-mode semiconductor laser diode (3SPhotonics 2000CHP), with a spot size of about  $80 \mu\text{m} \times 120 \mu\text{m}$  on the semiconductor chip surface. In this case, the QDH-VECSEL was able to deliver up to 16.3 mW at  $T=19.5^\circ\text{C}$  (still pump limited), with a multi-longitudinal mode emission centered at 1617 nm (not shown). In order to achieve single-frequency operation, a  $40 \mu\text{m}$ -thick fused silica etalon ( $R = 30\%$  on both faces) has been inserted inside the laser cavity, as presented in Fig. 1(d). As shown in Fig. 2(b), a CW maximum output power of 7.9 mW at  $T = 19.5^\circ\text{C}$  has been obtained, for an incident pump power of 1 W, and a single-frequency emission centered at  $\sim 1611$  nm (confirmed by the Fabry-Perot interferometer). In these conditions, we measured an orthogonal polarization suppression ratio of 23 dB between the two orthogonally polarized states aligned along the [1-

10] and [110] directions. The QDH-VECSEL is constantly polarized according to the [1-10] direction above laser threshold, as previously reported on QDH-based monolithic VCSEL [15,16]. By manually rotating the etalon, it was possible to tune the laser wavelength from 1609 nm to 1622 nm, while maintaining single-frequency emission.

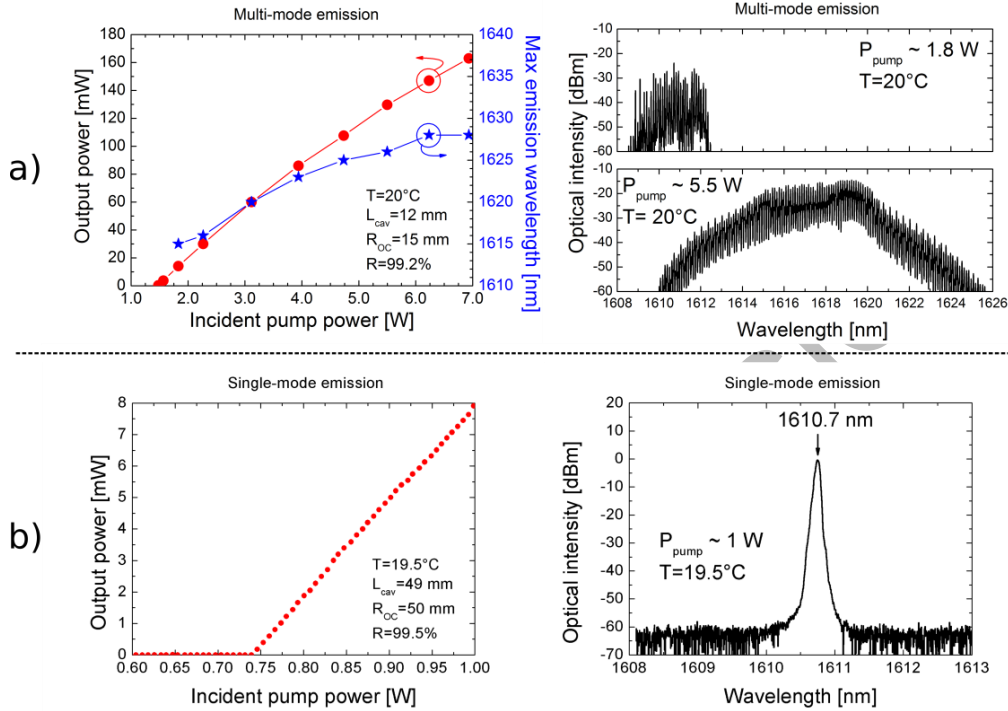


Fig. 2. Output power vs incident pump power characteristics (left) and emission spectra (right) of the OP-QDH-VECSEL in the case of (a) the multi-longitudinal mode and (b) the single-frequency operation.

In order to estimate the spectral purity of our OP-QDH-VECSEL, a delayed self-heterodyne linewidth measurement has been performed. To this purpose, an unbalanced Mach-Zehnder interferometer, which consists of an 80 MHz acousto-optic modulator on one arm and a 700 m delay line on the other arm, has been used [20]. Figure 3(a) shows the beat tone spectrum of our laser, obtained for a sweep time of 474 ms and a resolution bandwidth (RBW) of 10 Hz. The spectral linewidth of the OP-QDH-VECSEL is estimated from the pedestal portion of the autocorrelation spectrum while ignoring the broadened delta function in the middle. The wings of this spectrum are fitted by a Lorentzian function, which leads to an estimated linewidth of 22 kHz. This is a typical value for solid-state lasers and long-cavity VCSELs [21,22]. A more accurate measurement will be conducted in a future work using two identical lasers with long term stabilization on an Ultra-Low-Expansion (ULE) cavity. The two spurious peaks appearing at  $\pm 110$  kHz frequency offset are due to the acousto-optic driver electronics.

The same self-heterodyne bench has been used to characterize the frequency noise of the OP-QDH-VECSEL. To this aim, the signal provided by the photodiode is demodulated both in phase and in quadrature. The phase noise spectrum of the beating signal is thus numerically reconstructed. Figure 3(b) shows the phase noise of the OP-QDH-VECSEL obtained in free-running operation, for an acquisition time of 1 s. Above 10 kHz frequency offset, the phase noise is below -70 dBc/Hz and reaches -110 dBc/Hz at frequencies above 200 kHz. The peaks lying at 286 kHz (and its harmonics) correspond to the inverse of the self-heterodyne measurement delay time (and its multiples). It is worthwhile to notice that the spurious peaks

at  $\pm 110$  kHz are no more visible in the phase noise spectrum, proving that these peaks are related to additive intensity noise. The low-frequency excess noise below 10 kHz, which in particular induces the broadening of the delta function visible in Fig. 3(a), is mostly due to mechanical vibrations and thermal drift of the laser, as well as to thermal fluctuations of the decorrelation arm of the Mach-Zehnder interferometer.

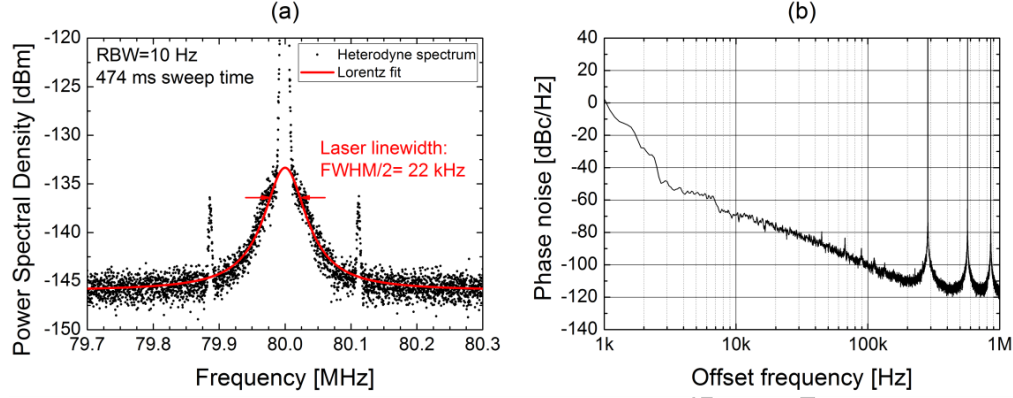


Fig. 3. (a) OP-QDH-VECSEL delayed self-heterodyne linewidth and (b) phase noise.

At this stage, it is important to characterize our laser in terms of Relative Intensity Noise (RIN) in order to precisely quantify the level of its noise versus frequency, but also, and most importantly, to explore its dynamical behavior which should reveal Class-A operation. To this aim, both QDH-VECSEL and pump diode signals have been acquired with a dedicated RIN measurement bench composed of a fibered InGaAs fast PIN photodiode (EPITAXX ETX 100 RFC2, 1 GHz bandwidth), a RF amplifier (MITEQ AU-1332, 54 dB amplification) and an RF Electrical Spectrum Analyzer (Rohde & Schwarz FSV3). The RIN spectra of the laser and the pump are reported in Fig. 4(a). They both exhibit resonant peaks which makes it difficult to assess the transfer function of the QDH-VECSEL. It turned out that these peaks were due the presence of the FBG in the fiber pigtail of the pump laser. Indeed, the FBG applies a small optical feedback to the pump, intended to stabilize its emission wavelength. These peaks are replicated at multiples of the inverse of the external cavity round-trip time  $\tau_{\text{ext}}$ , i.e. the free spectral range  $\Delta\nu = 1/\tau_{\text{ext}} = 32$  MHz, for a fiber cavity length  $L = 3.25$  m, as checked by inspection [23]. These peaks are then transferred to the OP-QDH-VECSEL RIN, spoiling the noise behavior, as shown in Fig. 4(a). To overcome this issue and recover a clear RIN curve for our VECSEL, the Bragg grating has been removed from the pump fiber. Accordingly, the pump RIN shows now a nearly white noise characteristic over the whole frequency range of interest (100 kHz – 100 MHz), with a value of -155 dB/Hz for a detected photocurrent of 1.26 mA (red curve in Fig. 4(b)). The pump wavelength is no more fixed, but it is stable enough to ensure a constant pumping rate over hours. The RIN spectrum of the VECSEL becomes smooth and exhibits a characteristic first-order low-pass filter shape, as shown in Fig. 4(b). The OP-QDH-VECSEL transfer function, which is obtained by normalizing the laser RIN by the pump RIN, is shown in Fig. 4(c). It is indeed a first-order low-pass filter, with a -20 dB/dec slope, which is a clear signature of the Class-A operation of our laser. The cut-off frequency is found to be about 800 kHz. As shown in Fig. 4(b), the laser RIN decreases above this frequency to reach the shot-noise floor at -158 dB/Hz, for an average detected photocurrent of 2 mA. The measured OP-QDH-VECSEL transfer function is fitted using the following expression [24]:

$$H(f) = \frac{\gamma_{\text{cav}}^2}{\left[ \gamma_{\text{cav}} \left( \frac{r-1}{r} \right) \right]^2 + [2\pi f]^2}. \quad (1)$$



where  $\gamma_{\text{cav}}$  is the cavity decay rate (inverse of the photon cavity lifetime  $\tau_{\text{cav}}$ ) and  $r$  is the pumping rate coefficient, which is equal to  $r = 1.39$  in our case. This fitting leads to a photon lifetime  $\tau_{\text{cav}} = 53$  ns, in agreement with the 0.6% estimated cavity losses per round-trip.

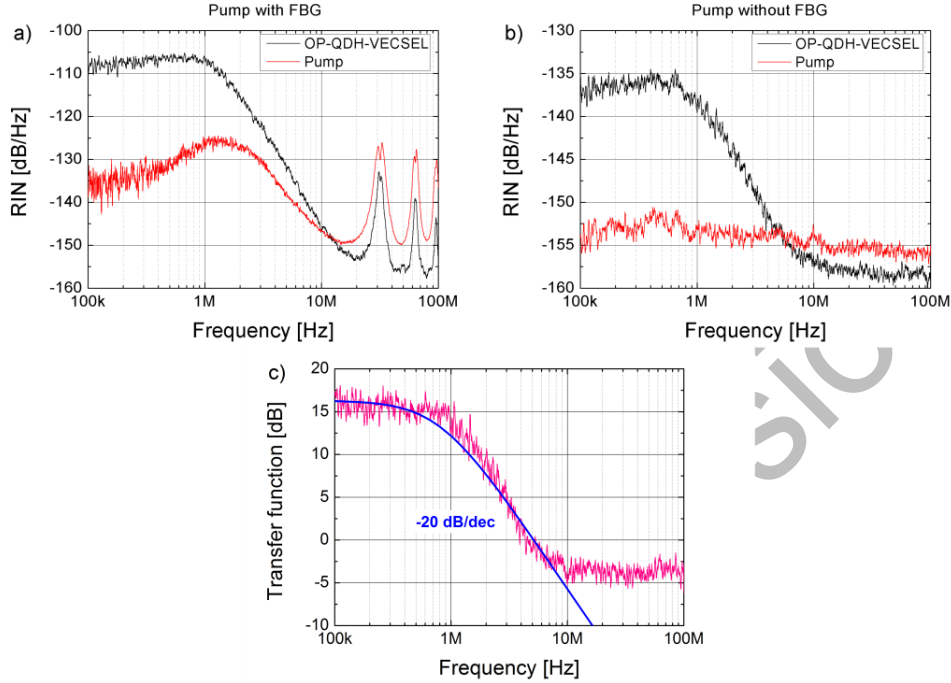


Fig. 4. RIN spectra of the OP-QDH-VECSEL (black curve) and the pump (red curve) with (a) and without (b) the FBG. (c) OP-QDH-VECSEL transfer function. RBW = 10 kHz.

### 3. Conclusions

In this paper we demonstrate a 1.6  $\mu\text{m}$ -emitting Optically-Pumped Vertical-External-Cavity Surface-Emitting Laser on InP, integrating an InAs Quantum Dash-based active region. The device has been characterized in two different cavity setups, allowing obtaining a maximum output power of 163 mW at 20°C in multi-transverse mode operation in a 12 mm-long cavity. When the laser is made single-frequency, the maximum measured output power is 7.9 mW at 19.5°C in a 49 mm-long cavity. In this condition, its wavelength is tunable from 1609 nm to 1622 nm. The laser linewidth has been estimated to be of about 22 kHz. Finally, Class-A operation is demonstrated with a cut-off frequency of 800 kHz. RIN levels of -135 dB/Hz at 100 kHz and below -158 dB/Hz (shot-noise limited) above 10 MHz are obtained. Further work includes a deepest investigation of the laser line characteristics for stabilization on ULE cavities, as well as possible dual-frequency operation of the OP-QDH-VECSEL.

### Funding

Agence Nationale de la Recherche (ANR) and Direction Générale de l'Armement (DGA) (ANR-ASTRID HYPOCAMP, grant ANR-14-ASTR-0007-01); DGA-MRIS and Région Bretagne (grant ARED-VELOCE 8917).